AUTOMATIC INTERPRETATION OF ULTRASONIC IMAGING*

Stephen S. Lane
Adaptronics, Inc.
McLean, Virginia 22102

and

Douglas K. Lemon
Battelle-Northwest
Richland, Washington 99352

ABSTRACT

The objective of this work is to develop an advanced automatic ultrasonic inspection system via adaptive learning network signal processing techniques. This system will provide the type, location, and size of defects in metal more quickly and to smaller defect size than current imaging systems, without the need for operator interpretation of the results.

An ultrasonic imaging array constructed for this project has been used to record data from artificial defects in carbon steel test blocks. Software has been written to automatically determine the orientation and size of cracks from these digitized waveforms. Detection of these cracks has been unambiguous down to 1/6 wavelength or 0.25 mm. Sizing for depth is accurate to 12% down to 1/3 wavelength.

Further research will extend these results to other defect types and to smaller defects. The significance of this work is that it will demonstrate the feasibility of a totally automatic detection, classification, and sizing system which will work with hardware ordinarily used for imaging. This system will provide a numerical estimate of the defect parameters rather than an image requiring operator interpretation, and it will do so at defect dimensions smaller than the limits set by the resolution of imaging systems.

INTRODUCTION

It is generally recognized that the ultrasonic energy pattern or signature reflected from a given target contains substantially greater information than is being utilized by present ultrasonic nondestructive testing techniques. When an ultrasonic sound beam illuminates a given target, the pattern generated by the target contains reflected, diffracted, and redirected energies which include time, amplitude, and frequency spectral information that uniquely describes the reflector. Linear arrays afford the opportunity of capturing the pattern reflected from a flaw or target.

It was anticipated at the start of this program that parameters of the scattered waveforms, as well as those of the reflected energy, could be used to size defects. This has proven to be the case as will be shown in this paper. Parameters from the mode-converted diffracted adaptive learning networks to classify these cracks as to their orientation and provide estimates of their depth. Furthermore, the work reported here shows that these parameters can be extracted from the raw waveforms automatically. It remains in this project to extend these results to other types of defects and to implement the algorithms developed so far in hardware.

DATA COLLECTION

The experimental apparatus has been described in last year's Proceedings of this conference[1] and only changes in that description will be presented here. All data were collected by D. K. Lemon of Battelle. The outboard array previously referred to was positioned as close as possible to the main receiving array, and receiving elements on the main array were wired as shown in Fig. 1. A shear (S) wave beam at 34° from the vertical was directed into the metal; pulse-echo data from the outboard array and pitch-catch data from receivers on the main array were collected for all EDM notches, both at 0° and 30° from the vertical. This constituted a total of 32 artificial defects. Data were taken on the main array for receivers successively further from the outboard array until no defect-related signal could be observed. Approximately 700 waveforms were recorded in this way. All defects were detected with good signal-to-noise ratio.

SOFTWARE DEVELOPMENT

Software to simulate, as far as possible, the intended functions of the ALN 4000 in this application was written to analyze these data. Since the array was positioned by an operator this function could not be simulated. In the hardware implementation, the ALN 4000 will acquire the desired waveforms by addressing particular receivers. Here, all waveforms were prerecorded and were acquired by searching through a list for the desired receiver. All other functions described below will be implemented in software much as they are here.

TRANSMIT/RECEIVE ARRAY #2   BEAMFORMING ARRAY   TRANSMIT/RECEIVE ARRAY #1

WATER LINE

TEST BLOCK
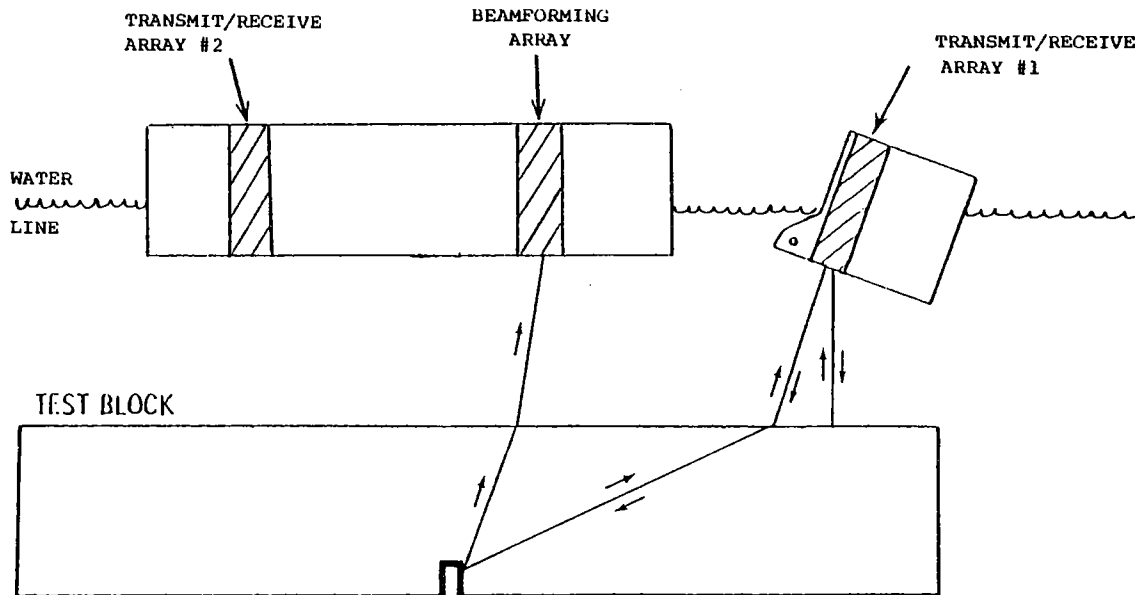
CURRENT		FUTURE	
Given:	Beam Angles	Given:	Beam Angles
	Two Water Depths, Steel Depth		Two Water Depths, Arrival Times
	Receiver-Transmitter Distance		Receiver/Transmitter Distance
Find:	Phase Arrival Time	Find:	Defect Depth

Fig. 1 Test block and ultrasonic arrays.

The system performs the following functions in this sequence:

- detect defect in pulse-echo mode;

- acquire pitch-catch waveforms;

- identify defect-related energy;

- extract features; and

- classify and size.

The specific implementation of these steps is shown in Fig. 2. Defect detection is performed by moving the array by a step size as determined by the ultrasonic spot size and acquiring a pulse-echo waveform. This waveform is passed to a signal detector which selects those portions of the waveform where the signal-to-noise ratio is high enough that a signal may be claimed to be present. The detection-association-processor (DAP) determines which, if any, of those signals may be due to a defect of interest. Other signals may be due to geometric reflectors or uninteresting defects such as layers of precipitate. If no defect is present, the array is moved to another nearby position. If a defect-related detection is found, the array is stopped and additional waveforms are acquired.

In the present configuration, eight waveforms from the receivers labeled "beamforming array" in Fig. 1 are recorded and used to form an ordinary time-delay-and-sum beam pointed at the defect at the compressional (P) wave velocity. The mode-
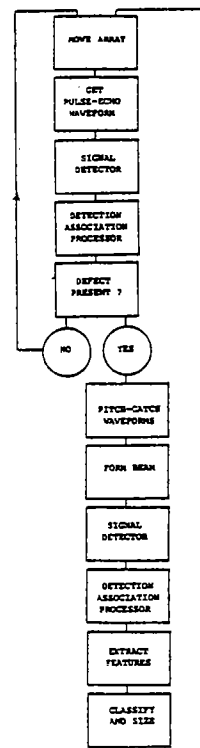

Fig. 2 Inspection system logic.

converted diffracted energy preferentially passed by this beam is expected to provide significant sizing and classification information. This beamed waveform proceeds to the signal detector which locates time windows with signals as before. The detection association processor again finds those signals due to the defect, and these signals provide the features used in classification and sizing, the last step in the process.

Figure 3 shows some details of the signal detector. The only reasonable criterion for the presence of a signal is a signal-to-noise ratio (DET) above some preassigned threshold, so the task of a signal detector is to calculate the noise power and the signal power. This is done by executing the loop shown in Fig. 3 once per time point. The signal power (STA) is simply the average power over some time window, generally about the length of the expected signal. The noise power (LTA) is the average power over some much longer time interval preceding the current time, and chosen so as to exclude any signals. The noise power as well as the signal power must be continually updated in order to account for the inevitable nonstationarity in the noise. Nonstationarity occurs for a variety of reasons in real experiments, and in this case is caused by distance-dependent attenuation and inhomogeneities in the metal, among others.
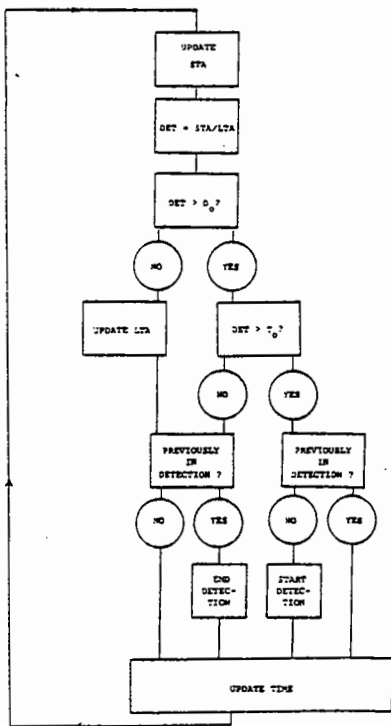

Fig. 3 Signal detector logic.

Bursts of noise of short duration may occur in the data, and these should not be included in the noise estimate. Neither should they be declared to be signals, so separate thresholds are set for freezing the noise estimate and for declaring detections. It is found that setting the detection threshold about 4 dB above the noise-freezing threshold does result in satisfactory performance. When the signal-to-noise ratio crosses the detection threshold, an entry is made in the detection log, claiming the beginning or ending of a signal, depending on whether the signal-to-noise ratio was increasing or decreasing.

Figure 4 shows a sample waveform from a beam of eight elements directed toward an EDM notch 0.76 mm deep. The waveform with windows where a detection was claimed is shown in the top of the figure, and the signal-to-noise ratio in the bottom. The horizontal line at the bottom corresponds to the detection threshold, about 18 dB in this case. Corresponding arrows on the top figure show detections. The predicted arrival time for the mode converted energy is indicated by "SP time" and is seen to agree well with the actual arrival time of a pulse of energy.

It is the task of the detection-association-processor (DAP) to predict the arrival times of the various phases and decide which, if any, of the actual detections match those times. It therefore must contain a model of the experiment, including distances, geometry, and propagation velocities. Figure 1 shows the relevant ray paths for this experiment.

First, the DAP calculates the water depth. There is sufficient side-lobe energy from the outboard array to give a large response from the front surface, and this enables the calculation of the water depth, given the speed of compressional waves in water. Then the phase arrival time can be found from the metal depth, the shear wave velocity in the metal, and the beam angle in the water bath. In the future when defects at different depths are examined, a depth will be calculated for each arrival time and those in the range of interest accepted as belonging to defects.

When the DAP is entered with a detection log from a pitch-catch waveform, the requirements are somewhat different. The water depth and the defect depth are known, and it is required to find the arrival times of the various phases at a given receiver. Again, from Fig. 1 it can be seen that knowledge of the geometry, the transmitter-receiver distance, and the various velocities may be used to find these times. The signal closest in time to the predicted time, if it is within a preset tolerance, will be claimed to be the phase in question.

FEATURE EXTRACTION

Once the required signals were obtained, parameters were extracted. Previous experience (Shankar, 1979)[2] has shown that spectral parameters may be used to size cracks ultrasonically. Accordingly, power spectra of all arrivals were calculated and the parameters illustrated in Fig. 5 found. This figure shows the power spectrum of the SP waveform shown in Fig. 4 and is typical of SP phases. The frequency interval between 0.5 and 4.0 MHz has been divided into eight equal intervals, and the fractional power in each interval calculated. These powers are normalized parameters not dependent on gains or pulser settings. The integral of this parameter, i.e., the power in a band up to and including a particular frequency, was also calculated. Finally, the frequency at which the integrated fractional power achieved 1/8, 2/8, ... was found.

Predicted SP Time

Time in microseconds

$$Det = \frac{Short\text{-}term\ average\ Power}{Long\text{-}term\ average\ Power}$$

Time in microseconds

Fig. 4   Beamed waveforms.

Frequency, MHz
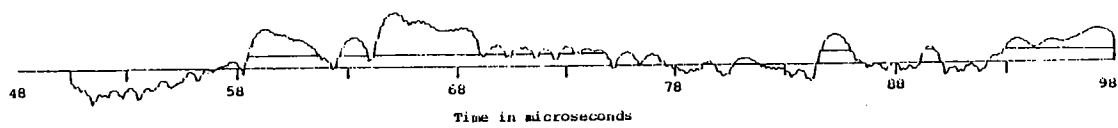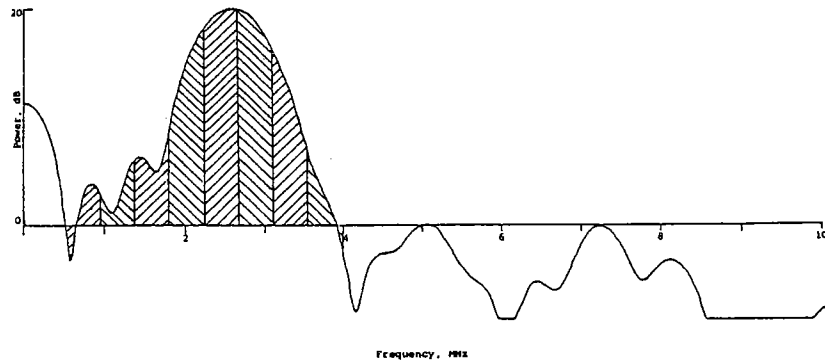
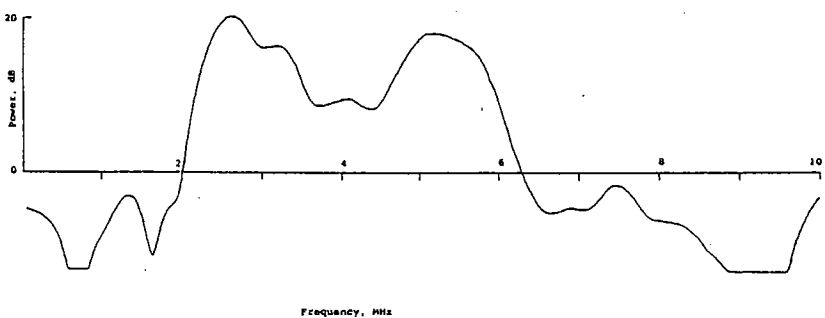Fig. 5   SP power spectrum.

Frequency, MHz

Fig. 6   SS power spectrum.

These parameters describe the shape of the spectrum. The first indicates the location of the spectral peak. The second, the integrated power, gives an idea of how sharply peaked the spectrum is. Rapid variation in this parameter indicates a narrow spectrum. The third has the opposite meaning. Large changes in this parameter indicate a slowly varying spectrum. As a group, they were found satisfactory for parameterizing the spectrum.

Figure 6 shows a typical SS spectrum recorded in the pulse-echo mode. The target was the same as that in Fig. 5, but the spectral shape is dramatically different. There is relatively much more energy in the frequency range above 4.0 MHz in the SS spectrum.

These spectra are as recorded so they contain the effects of the transducer, whose spectrum peaks at about 2.5 MHz and has a minor peak near 5.0 MHz. The energy in this minor peak is relatively less than its contribution in the SS spectrum, suggesting that the processes of mode conversion and diffraction at the target have shifted energy from the incident shear wave into the outgoing compressional wave much more efficiently at low frequencies than at high frequencies. Hence the low frequency SS level is lower than expected and the low frequency SP level higher than expected.

602

ADAPTIVE LEARNING NETWORKS

The SS spectra were parameterized in the same way as the SP spectra, except that the frequency range used was from 1.0 MHz to 6.5 MHz, reflecting the different distribution of energy in these spectra. All spectral parameters were input to Adaptronics adaptive learning network software which found networks which discriminated between cracks at 30° and 0° from the vertical, and which found the depths of the cracks in each class. Separate networks were necessary for each crack angle, a result that might be expected given the fact that discrimination on angle was possible. Networks for classification and sizing are shown in Figs. 7, 8, and 9, along with the parameters involved in them. In every case, parameters from the SP waveforms were found to be important, showing that mode-converted and diffracted energy is indeed useful in defect characterization. Finally, Fig. 10 shows the model depth as a function of the true depth for both crack orientations. The mean absolute deviation between model and prediction is about 12% here, which is satisfactory agreement.

SUMMARY AND CONCLUSIONS

Using the present array and software, present capability is:

- cracks can be detected automatically and unambiguously as low as 1/6 wavelength;

- cracks at 30° from the vertical can be distinguished from those at 0° from the vertical;

- cracks can be sized with about 12% mean deviation from the true depth as low as 1/3 wavelength; and

- the processes for acquiring the data to train the adaptive learning networks for these functions can be made automatic, as can be actual sizing and classification themselves.

REFERENCES

1. A. N., Mucciardi, S. S. Lane, and G. J. Posakony, "Overview of Planned Ultrasonic Imaging System with Automatic ALN Data Interpretation, "DARPA Contract DSA MDA 903-78-C-0223, March 15, 1978 to May 14, 1980.

2. R. S., Shankar, in EPRI NP-964 1979 Interim Report, January 1979, on EPRI Contract RP1125-1, Application of Nonlinear Signal Processing to Pipe and Nozzle Inspection.
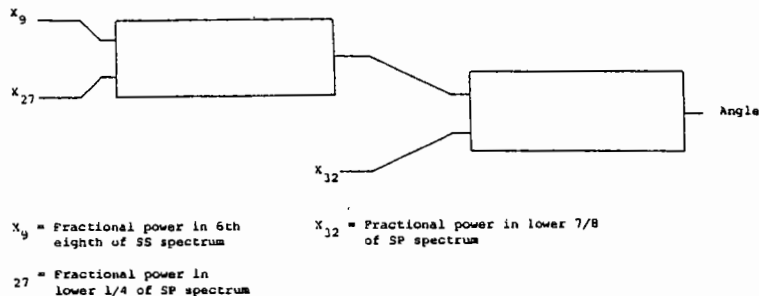
X_9 = Fractional power in 6th eighth of SS spectrum

X_{27} = Fractional power in lower 1/4 of SP spectrum

X_{12} = Fractional power in lower 7/8 of SP spectrum

Fig. 7 Network to discriminate crack angle.

X_6 = Power in 3rd eighth of frequency band for SS

X_{13} = Power in 4th eighth of frequency band for SP

Fig. 8 Network to size 30° cracks.

X_1 = Fractional power in lower 3/4 of SP spectrum

X_3 = Frequency at which 1/4 of SP power is attained

X_{21} = Fractional power in lower 1/2 of SS spectrum
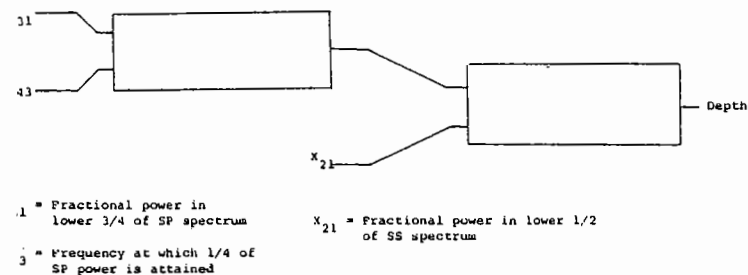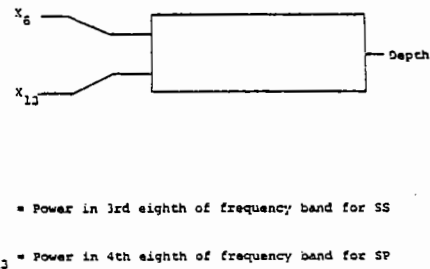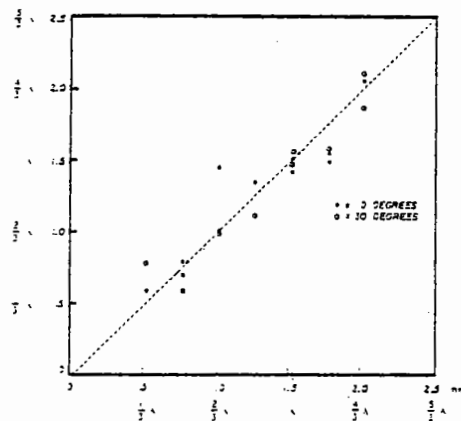
Fig. 9 Network to size 0° cracks.

Fig. 10

Predicted versus known crack depths

603

SUMMARY DISCUSSION
(S. S. Lane)

Mark Weinberg (U.S. Army Armament R&D Command): Were all three transducers fixed in relation to each other in the scan?

Steve Lane: They were in this experiment. There is a capability of moving the transducer array, number one, which is mounted on a goniometer to about five different known positions from the main array.

Mark Weinberg: Do you see any particular difficulty in applying a sequence of this nature to other than a flat plane?

Steve Lane: The detection association processor would have to be modified to correctly predict the mode arrival times. But other than that, no. You would also have to know where you were with respect to the curved front surface, for instance. But presumably the pulse echo shots at the front surface could give you that information.

# #